



Research articles

Magneto-impedance Effects in Electrodeposited Multi-layer [NiFe/Cu]₃ on Cu Wire Substrates for kHz–order Frequency Measurements

Blasius Anggit Wicaksono¹, Nuryani², Budi Purnama^{2*}¹Department of Physics Education, Faculty of Education, University of Lampung, Jl. Prof. Dr. Ir. Sumantri Brojonegoro St., No. 1, Bandar Lampung, Lampung 35141 Indonesia²Physics Department, Universitas Sebelas Maret, Ir. Sutami St., No. 36A, Surakarta, 57126, Indonesia

Article info

Keywords:

[NiFe/Cu]₃
Magneto-impedance
Electrodeposition
Multi-layered system
Saturation magnetization

Abstract

The magneto-impedance effect (MI) in an electrodeposited multi-layered system of [NiFe/Cu]_N on a Cu wire was modified by varying the thickness of the Cu spacer layer. The multi-layered samples of [NiFe/Cu]_N were deposited by the electrodeposition using a platinum electrode. The MI ratio rapidly increased with a frequency of up to 100 kHz where it saturated. Conversely, the MI ratio of the multi-layered system [NiFe (800 nm)/Cu(y nm)]₃ was a decreasing function of Cu layer thickness. The decreased MI ratio may be attributed to the lowered saturation magnetization in the multi-layered system with thicker spacer layers.

1. Introduction

The electrical impedance of some ferromagnetic material greatly changes under an external magnetic field [1]. Such phenomenon is known as magneto-impedance (MI). The MI effects play an important role in modern technology. In particular, they are exploited in variable magnetic sensors for ultra-low magnetic field applications such as cardiac magnetic activity detectors [2–5]. Atalay and Atalay investigated the effect of MI in a single-layered NiFe of different thicknesses on Cu wire substrate. They reported a significant effect of NiFe thickness on the MI ratio. The MI effect is also sensitive to the high frequency, such as much larger than megahertz order [6].

The complex impedance is expressed as $Z = R + iX$, where R is the resistance (real part) and X is the reactance (imaginary part). The magnitude of the MI ratio ($\Delta Z/Z$) under an external field H is expressed in Eq. 1:

$$\frac{\Delta Z}{Z} (\%) = \frac{Z(H) - Z(H_{max})}{Z(H_{max})} \times 100\% \quad (1)$$

where $Z(H)$ is the measured impedance ($|Z|^2 = R^2 + X^2$) in the absence of the magnetic field (i.e., $H = 0$) and $Z(H_{max})$ is the impedance at the maximum external magnetic field (H) [7], i.e., threshold magnetic field required for saturated impedance.

Theoretically, the MI effect depends on the skin effect in the magnetic conductor [8]. In turn, the skin effect is related to the skin depth i.e., the penetration depth δ_m of the electromagnetic waves. The skin depth is the depth below the surface of the conducting wire at which B and H are 37% lower than at the conductor surface [9]. The magnitude δ_m of the conducting wire is a function of the circumferential permeability (μ_ϕ) and is given by Eq. 2:

$$\delta_m = \frac{c}{\sqrt{4\pi^2 f \sigma \mu_\phi}} \quad (2)$$

where c is the speed of light, σ is the electrical conductivity, and $f = \omega/2\pi$ is the frequency of the alternating currents flowing through the sample.

The multi-layered structure consists of N repeats of two magnetic layers separated by non-magnetic-spacer layers. The impedance of multi-layer structure is given by Eq. 3:

$$Z = R_m \left(1 - 2j\hat{\mu}_{yy} \frac{d_1 d_2}{\delta_1^2} \right) \quad (3)$$

where $R_m = l/2\sigma_1 d_1 b$ is the resistance of the conductor layer, $\delta_1 = c/\sqrt{2\pi\sigma_1\omega}$, is the skin depth inside the conductive layer, and $\hat{\mu}_{yy}$ is the permeability tensor, d_1 and d_2 are the thickness of the spacer and magnetic layers, respectively. As per Eq. (3), the MI ratio of multi-layer configuration enhanced at the low frequency when the skin depth effect is not subdued and is a linear function of $\hat{\mu}_{yy}$ [10].

This study aimed to demonstrate the modulation of MI in a multi-layered structure. The magnetic layers are permalloy thin films of NiFe interdigitated with Cu film to form multi-layered structures [NiFe/Cu]_N where $N = 3$ is the repetition number and the Cu films are conducting spacer layers. Whole films were fabricated by electrodeposition on the wire substrate with modification by the thickness of the spacer layer.

2. Experimental Methods

The multi-layer structure of [NiFe(800 nm)/Cu(y)]₃ with $y = 0, 100, \text{ and } 200$ nm used in this experiment was fabricated by electrodeposition with a platinum wire electrode. The substrates were copper wires (diameter = 0.46 mm). Before electrodeposition, the substrate was cleaned with ultrasonic cleaners. The electrolyte baths used in the electrodeposition of the multi-layer structure [NiFe/Cu]_N are listed in Table 1. The electrolyte bath solution was adjusted to a constant pH 2.7 by adding up to 0.05 ml of 1 M H₂SO₄.

*Corresponding author
Email: bpurnama@mipa.uns.ac.id

Table 1. Electrolyte bath used in the multi-layer [NiFe/Cu]_N deposition

Desired Layer	Electrolyte bath	Concentration
NiFe	NiSO ₄ ·6H ₂ O	0.099 M
	FeSO ₄ ·7H ₂ O	0.012 M
	H ₃ BO ₄	0.149 M
	C ₆ H ₈ O ₃	0.002 M
Cu	CuSO ₄ ·5H ₂ O	0.065 M
	C ₆ H ₁₂ O ₆	0.002 M

The electrodeposition rates of NiFe and Cu spacer layers were 2 nm/s and 6 nm/s, respectively, achieved at current densities of 15.5 mA/cm² and 8 mA/cm², respectively. By repeating this electroplating process, we fabricated multi-layered structures [NiFe(800 nm)/Cu(y)]₃ with y = 0, 100 and 200 nm. The element compositions of the obtained multi-layer samples were characterized by X-ray fluorescence and their crystalline structures were determined by X-ray diffraction (data not shown). The magnetic characteristics were measured by a vibrating sample magnetometer (VSM). The magnetic dependence of the impedance (MI) was then measured by a conventional LCR meter as shown in Figure 1. The magnitude of the measured impedance was calculated as the square root of the sum of the squared real (resistance) and imaginary (reactance) component ($Z = \sqrt{R^2 + X^2}$).

The MI data were obtained by measuring the resistance value (R) and reactance (X) while varying the external field H.

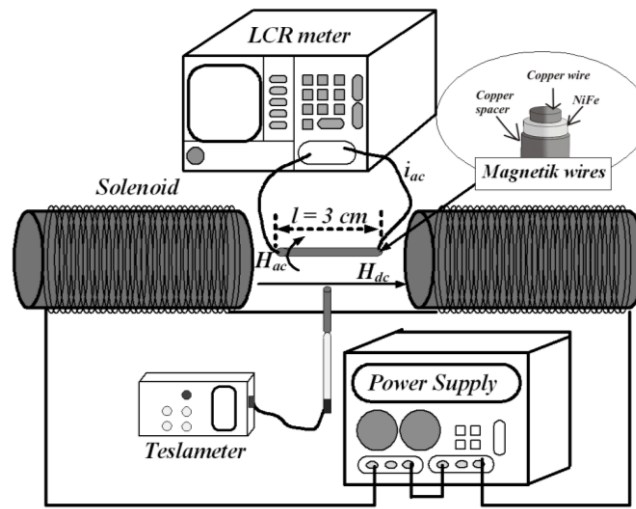


Fig. 1. Experimental schematic of the measurement of MI effects

3. Results and Discussion

Figure 2 plot the MI ratio as a function of frequency *f*. The characteristic MI curves in Figure 2(a) were obtained under an external magnetic field *H* with *f* = 20 kHz and 100 kHz. Evidently, the shape of the MI versus *H* plot is identical at two frequencies, and the MI ratio maximized at *H* = 0. The MI ratio rapidly decreased as *H* increased up to ±40 mT and became almost constant thereafter. The magnitude of *H* beyond which the MI ratio no longer changes was not significantly different between *f* = 20 kHz and 100 kHz. However, the peak MI ratio significantly increased from 36.5% at *f* = 20 kHz to 54.4% at *f* = 100 kHz. The type of the MI ratio as a function of frequency is depicted in Fig 2(b), i.e., for *f* = 20 kHz and 100 kHz. Other frequency also has a similar profile of the MI curve. It notes that the value of MI rapidly increased up to *f* = 40 kHz and it thereafter tended to saturate. The MI realization at low frequency indicates that the MI support dominantly by the inductive component [2]. The obtained results are consistent with those of Mishra [5].

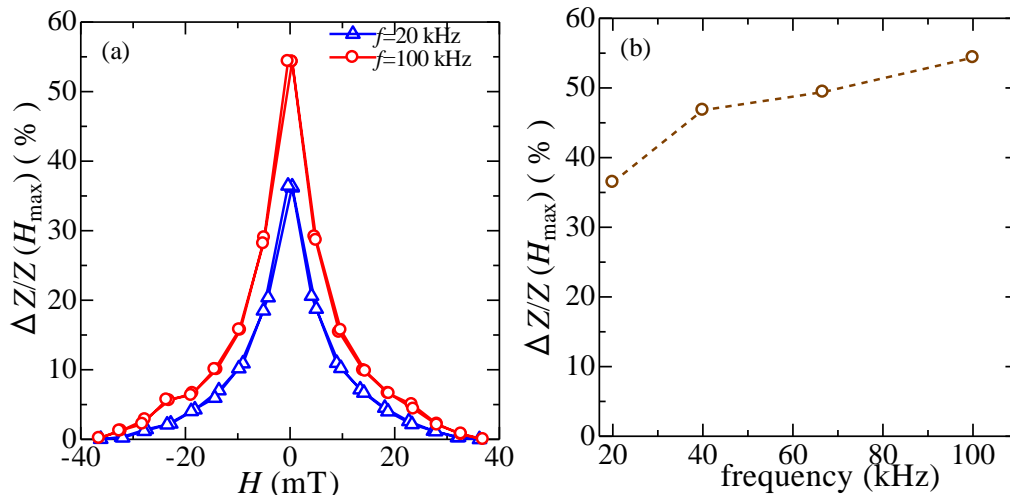


Fig. 2. (a) The typical MI versus *H* curves for multi-layered [NiFe₈₀Fe₂₀(800 nm)/Cu(300 nm)]₃ at applied frequencies of 20 kHz (triangles) and 100 kHz (circles) (b) MI ratio versus frequency.

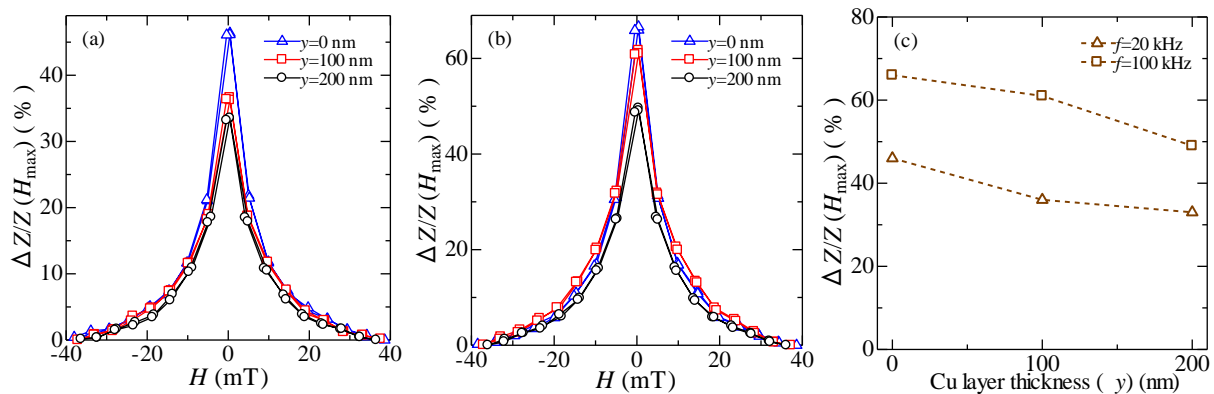


Fig. 3. Typical MI versus H curves for a thin layer of $[\text{NiFe} (800 \text{ nm})/\text{Cu} (y \text{ nm})]_3$ with different thickness of the Cu spacer layer at (a) 20 kHz and (b) 100 kHz; (c) MI ratio versus Cu thickness at applied frequencies of 20 (triangles) and 100 kHz (squares)

The MI characteristics are further explored in Fig. 3. Panels (a) and (b) of this figure plot the characteristic MI curves of the multi-layered structure $[\text{NiFe} (800 \text{ nm})/\text{Cu} (y \text{ nm})]_3$ under a magnetic field H at frequencies 20 and 100 kHz, respectively. In this plot, the thickness y of the Cu spacer layers is varied as 0, 100, and 200 nm. As shown in Fig. 3(a), the MI curve of the multi-layer $[\text{NiFe} (800 \text{ nm})/\text{Cu} (y \text{ nm})]_3$ is similarly shaped at all Cu thickness. However, the spacer layer affects the maximum MI ratio. The MI ratio was 46.36% in the absence of the spacer layers ($y = 0$ nm), decreasing to 36.41% for $y = 100$ nm. When the Cu thickness was doubled ($y = 200$ nm), the MI ratio further reduced to 33.55%. Similar results were also observed at $f = 100$ kHz (Figure 3(b)), but the MI ratio were much larger than at 20 kHz being 66.61%, 61.69% and 49.62% for $y = 0, 100, 200$ nm respectively.

Figure 3 (c) plots the maximum MI ratios determined from panels (a) and (b) as a function of spacer layer thickness. This plot clarifies the decrease in MI ratio with increasing thickness of Cu spacer layer in the multi-layer structure $[\text{NiFe} (800 \text{ nm})/\text{Cu} (y \text{ nm})]_3$. To explain these interesting results, the multi-layered structure $[\text{NiFe} (800 \text{ nm})/\text{Cu} (y \text{ nm})]_3$ was magnetically characterized by VSM. The magnetic characteristics are presented in Fig. 4. The saturation magnetization M_s was 877 emu/cm^3 at $y = 0$ and decreased with increasing thickness of the Cu spacer layer. M_s reduced to 525 emu/cm^3 at $y = 100$ nm and it further reduced to 443 emu/cm^3 at $y = 200$ nm. Therefore, the reduction in the MI ratio as the spacer layer widens can be correlated to the decreased M_s .

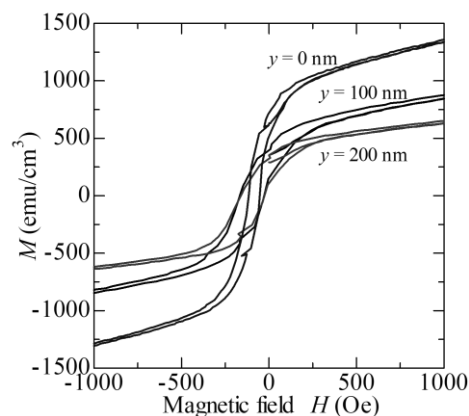


Fig. 4. Multi-layer hysteresis curve of $[\text{NiFe}(800 \text{ nm})/\text{Cu}(y \text{ nm})]_3$ with variations of y , i.e., 0, 100, and 200 nm

4. Conclusions

This study investigated the MI effect in multi-layered systems of $[\text{NiFe}/\text{Cu}]_3$ electrodeposited on Cu wires. The MI ratio was modified by varying the thickness of the Cu spacer layer. The multi-layered samples of $[\text{NiFe}/\text{Cu}]_N$ were deposited by electrodeposition using a platinum electrode. The MI ratio rapidly increased to approximately 47% as the applied frequency increased to 40 kHz and it remained somewhat constant thereafter. In the multi-layered system of $[\text{NiFe}(800 \text{ nm})/\text{Cu}(y \text{ nm})]_3$, the MI ratio decreased with the increasing thickness of the Cu layer. The decreased MI ratio may be correlated to the lowering of the saturated magnetization in multi-layer systems with thicker Cu spacer.

Acknowledgements

This research was funded by Penelitian Unggulan Perguruan Tinggi, DIPA PNPB Universitas Sebelas Maret, Kementerian Riset, Teknologi, dan Pendidikan Tinggi, The Republic of Indonesia, contract No. 452/UN27.21/PN/2020.

References

- [1] P. Ripka, "Magnetic sensors and magnetometers," *Meas. Sci. Technol.*, vol. 13, no. 4, p. 645, 2002.
- [2] M.-H. Phan and H.-X. Peng, "Giant magnetoimpedance materials: Fundamentals and applications," *Prog. Mater. Sci.*, vol. 53, no. 2, pp. 323–420, 2008.
- [3] S. Nakayama, K. Sawamura, K. Mohri, and T. Uchiyama, "Pulse-Driven Magnetoimpedance Sensor Detection of Cardiac Magnetic Activity," *PLoS One*, vol. 6, no. 10, p. e25834, Oct. 2011.
- [4] M. Tejedor, B. Hernandez, M. L. Sanchez, V. M. Prida, and M. Vazquez, "Magneto-impedance effect in amorphous ribbons for stress sensor application," *Sensors Actuators A Phys.*, vol. 81, no. 1–3, pp. 98–101, 2000.
- [5] A. C. Mishra, "Microstructure, magnetic and magnetoimpedance properties in electrodeposited NiFe/Cu and CoNiFe/Cu wire with thiourea additive in plating bath," *Phys. B Condens. Matter*, vol. 407, no. 6, pp. 923–934, Mar. 2012.
- [6] F. E. Atalay and S. Atalay, "Giant magnetoimpedance effect in NiFe/Cu plated wire with various plating thicknesses," *J. Alloys Compd.*, vol. 392, no. 1–2, pp. 322–328, 2005.
- [7] M. Knobel, M. Vázquez, and L. Kraus, "Giant magnetoimpedance," *Handb. Magn. Mater.*, vol. 15, pp. 497–563, 2003.
- [8] C. García, J. M. Florez, P. Vargas, and C. A. Ross, "Asymmetrical giant magnetoimpedance in exchange-biased NiFe," *Appl. Phys. Lett.*, vol. 96, no. 23, p. 232501, Jun. 2010.

- [9] B. D. Cullity and C. D. Graham, "Introduction to Magnetic Materials, A John Wiley & Sons," *Inc., Hoboken, New Jersey*, p. 361, 2009.
- [10] L. V Panina and D. P. Makhnovskiy, "Magneto-impedance in multilayered films for miniature magnetic sensors," in *Introduction to Complex Mediums for Optics and Electromagnetics*, SPIE Press, 2003, pp. 267–291.